Terpyridine complexes of first row transition metals and electrochemical reduction of CO to CO.

Noémie Elgrishi, Matthew B Chambers, Vincent Artero, Marc Fontecave

Terpyridine complexes of first row transition metals and electrochemical reduction of CO_2 to CO

Noémie Elgrishi[a], Matthew B. Chambers[a], Vincent Artero[b] and Marc Fontecave[a,]*

Received (in XXX, XXX) Xth XXXXXXXXX 20XX, Accepted Xth XXXXXXXXX 20XX
DOI: 10.1039/b000000x

Homoleptic terpyridine complexes of first row transition metals are evaluated as catalysts for the electrocatalytic reduction of CO_2. Ni and Co-based catalytic systems are shown to reduce CO_2 to CO under the conditions tested. The Ni complex was found to exhibit selectivity for CO_2 over proton reduction while the Co-system generates mixtures of CO and H_2 with CO:H_2 ratios being tuneable through variations of the applied overpotential.

Introduction

The development of new energy storage technologies is central to solving the challenges facing the widespread use of renewable energies, namely their dilution and intermittent nature.[1,2] Batteries and hydrogen production are potential solutions which have been extensively investigated, but typically suffer from poor graviometric energy densities for the former and poor volumetric energy densities for the latter.[3] A more attractive option is the reduction of carbon dioxide (CO_2) into carbon-based fuels, combining higher graviometric and volumetric energy densities. This can be accomplished either directly through the generation of formic acid, methanol and higher hydrocarbons, or indirectly via the formation of carbon monoxide, which can be used as a feedstock chemical for the synthesis of alkanes through the Fischer-Tropsch process. Moreover, CO_2 reduction presents the advantage of providing a global carbon neutral energy system, fitting into existing infrastructure and facilitating energy transport.[4] This process can be achieved within an electrochemical cell in which electricity derived from renewable energy sources is converted into chemical energy.[5] However, the electroreduction of CO_2 generally requires the presence of catalysts and the application of large overpotentials, since the reactions involve multiple electrons. Furthermore it suffers from limited selectivity since a mixture of the products mentioned above are generally obtained, together with hydrogen (H_2), derived from the parallel reduction of protons required for activation of CO_2. Molecular compounds have proven to be beneficial to the understanding of structure-activity relationships and the optimization of electrocatalytic systems.[6,7,8] A challenging goal is the development of selective, efficient and cheap catalysts. Cost limitation would require the combination of simple and robust ligands with first row transition metals.

Polypyridine ligands, such as bipyridine (bpy) and terpyridine (tpy), are common ligands in coordination chemistry and molecular catalysis as they generally generate stable well-defined complexes.[9,10] As a consequence they have been frequently studied in the context of CO_2 electroreduction in organic solvents, most often acetonitrile (CH_3CN) or *N*,*N*-dimethylformamide (DMF), in the presence of a source of protons.[11] Such systems are capable of undergoing multiple reductions and thus storing multiple redox equivalents both in the ligand and in the metal ion.[12,13] Surprisingly, little has been done using synthetic metal-polypyridine complexes with first row transition metals. Indeed, the best reported catalysts are based on Re,[14,15,16] Rh[17,18,19] and Ru,[20,21] using mostly bpy and only in a few cases tpy ligands. Recently, [Mn(bpy-R)$(CO)_3$Br] (where bpy-R = substituted 2,2′-bipyridines) complexes were reported as electrocatalysts for the reduction of CO_2 to CO with reasonable efficiency, selectivity and stability.[22,23]

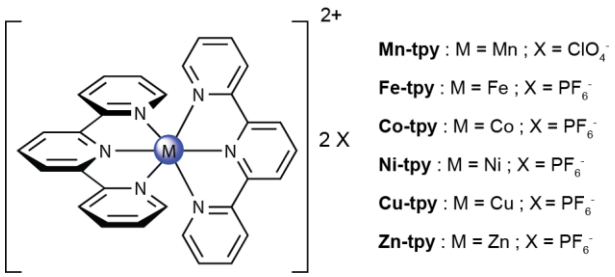

Scheme 1 Schematic depiction of the compounds studied.

Here we report on our investigation of $[M(tpy)_2]^{2+}$ systems, with M = Co, Ni, Zn, Mn, Cu, Fe (noted **M-tpy** in the following, see Scheme 1) as, to our surprise, these complexes were incompletely characterized as electrocatalysts for CO_2 reduction in solution. In fact these systems were studied at the end of the 80's by Abruna and collaborators almost exclusively in a different context, namely that of electrodes modified with electropolymerized films of vinyl-tpy-M complexes.[24,25,26,27,28] Here, on the basis of the first complete electrochemical characterization of **M-tpy** complexes, we show that: (i) **Co-tpy** and **Ni-tpy** complexes display electrocatalytic

properties for reduction of CO_2 into CO; (ii) within these complexes, polypyridine ligands such as tpy are highly susceptible to deleterious reactions which can explain the limited faradic yields.

Results

General experimental conditions

All metal-terpyridine complexes were synthesized and characterized according to reported procedures. Schematic depictions of **M-tpy** are shown in Scheme 1. Standard protocols for cyclic voltammetry and controlled-potential couloumetry experiments involved the use of DMF as a primary solvent in the presence of 0.1 M TBAP (tetra-*n*-butylammonium perchlorate) and 5% water as a source of protons, under CO_2-saturated conditions. The same bulk electrolyses experiments performed in CH_3CN as the primary solvent yielded comparable results, with the exception that some precipitate was observed. Following that which has been reported by Meyer and co-workers on analogous Ru polypyridyl systems, this precipitate is being tentatively assigned to be the result of reduced complex-carbonate/bicarbonate salts.[21] No evidence of precipitation was observed in DMF and thus, in order to limit side phenomena, DMF was used as the primary solvent for the studies reported herein. Since DMF can be subject to hydrolysis to yield formate or formaldehyde that is not derived from CO_2 reduction,[29] great attention was paid to the product analysis in control experiments.

As shown in the supplementary information section, similar results were obtained when synthetic $[M(tpy)_2]^{2+}$ complexes are replaced by a 1:2 mixture of the corresponding metal salt and the terpyridine ligand, respectively. All electrochemical potential values are reported relative to that of the ferrocenium/ferrocene couple under the conditions used. The IUPAC convention is used to report current.

Cyclic voltammetry

To assess the reactivity of **M-tpy** (M = Mn, Fe, Co, Ni, Cu) compounds towards CO_2 at reducing potentials, cyclic voltammetry experiments were carried out in DMF/H_2O (95:5, v:v) solutions of each complex, in Ar and CO_2-saturated conditions, with 0.1 M of TBAP as the supporting electrolyte. Identical conditions were used for **Zn-tpy** except a 90:10 volumetric solvent ratio was used.

Co-tpy

The cyclic voltammogram under Ar of a 2 mM solution of **Co-tpy** in a DMF/H_2O (95:5, v:v) mixture with 0.1 M TBAP displays two reversible one-electron electrochemical features in the –0.5 to –2.3 V *vs.* Fc^+/Fc range (Figure 1a, I and II). The first feature, at –1.17 V *vs.* Fc^+/Fc, is a reversible metal-based process, assigned to a Co^{II}/Co^{I} reduction (Figure 1a, II). This system is diffusion controlled, with a difference between the potential of the anodic and cathodic peaks (peak-to-peak separation) of about 60 mV at slow scan rates (59 to 64 mV in the 10-100 mV/sec range). The peak-to-peak separation then increases as the scan rate is further increased to reach a separation of 77 mV at a scan rate of 500 mV/sec. The plots of i_{pc} and i_{pa} *vs.* $v^{1/2}$ are linear and the i_{pa}/i_{pc} ratio is close to unity in the 10-500 mV/sec scan rate range (Figure S1). This feature was used to determine the diffusion coefficient using the Randles-Sevick equation. A diffusion coefficient of $3.7 \cdot 10^{-6}$ cm²/s was calculated. The second electrochemical feature, at –2.03 V *vs.* Fc^+/Fc, is attributed to a one-electron ligand-based reduction (Figure 1a, I). This couple is mostly reversible, with a peak-to-peak separation of about 66 mV for scan rates in the 10-50 mV/sec range. This value increases to 91 mV at 1 V/s. Plots of i_{pc} and i_{pa} versus $v^{1/2}$ are linear over the range of scan rates studied, and the i_{pa}/i_{pc} value is close to 1 which denotes chemical reversibility (Figure S1).

As the potential range interrogated was increased to include more anodic potentials, 0 V *vs.* Fc^+/Fc, a third feature at –0.17 V *vs.* Fc^+/Fc is observed and is attributed to the Co^{III}/Co^{II} couple (Figure 1a, III). If the potential window scanned is increased to more cathodic potentials values, an electrochemically irreversible wave is observed with a peak potential of –2.46 V *vs.* Fc^+/Fc (Figure S2). This wave is accompanied by the apparition of two anodic features at –1.54 and –0.76 V *vs.* Fc^+/Fc as well as a decrease in the intensity of the anodic waves of the Co^{II}/Co^{I} and tpy/$tpy^{\bullet -}$ couples. While investigating the lower potential ranges, as the number of scans is increased, the intensity of the anodic features of these two peaks continues to decrease. This additional irreversible feature at –2.46 V *vs.* Fc^+/Fc is attributed to a second ligand-based reduction and appears to lead to decomposition pathways. Therefore, the potential has always been controlled in the following work so as to avoid this deleterious reduction feature.

When the same solution was saturated with CO_2, no difference was observed in the metal-based processes (Figure 1a, II and III). A strong enhancement of the cathodic current was observed in the ligand-based reduction process, with an onset at –1.80 V *vs.* Fc^+/Fc as can be seen in Figure 1a. The current increases over 4 folds, from –0.33 to –1.51 mA/cm² (at –2.23 V, for a scan rate of 100 mV/s), and is stable over time. The wave becomes irreversible, with no anodic return-wave observed in the range of scan rates studied (10-1000 mV/sec, Figure S1). It is thus assigned to catalytic CO_2 reduction, which was confirmed by controlled potential electrolysis experiments.

Ni-tpy

Cyclic voltammograms of a 2 mM solution of **Ni-tpy** under inert atmosphere displays two reversible and diffusion-controlled electrochemical features at –1.62 and –1.88 V *vs.* Fc^+/Fc (Figure 1b, II and III). Both features are assigned to ligand-based electrochemical processes. Peak-to-peak separation of both features are close to 60 mV (62 and 65 mV respectively at 100 mV/s) and the plots of i_{pc} and i_{pa} *vs.* $v^{1/2}$ (Figure S3) are linear in the scan range studied (10-1000 mV/s), consistent with electrochemical and chemical reversibility.

At slow scan rates (10-20 mV/s), an additional small anodic feature is observed at –1.78 V *vs.* Fc^+/Fc (Figure S4). This observation might be explained if slow chemical event is invoked, such as the loss of a tridentate tpy ligand, which is not observed at faster scan rates.

Under CO_2-saturated conditions, the two electrochemical features lose reversibility (no anodic return feature is observed) and the intensity of the corresponding cathodic peaks increase over

2 fold, suggesting possible electrocatalytic behavior. A third irreversible catalytic cathodic wave is observed at lower

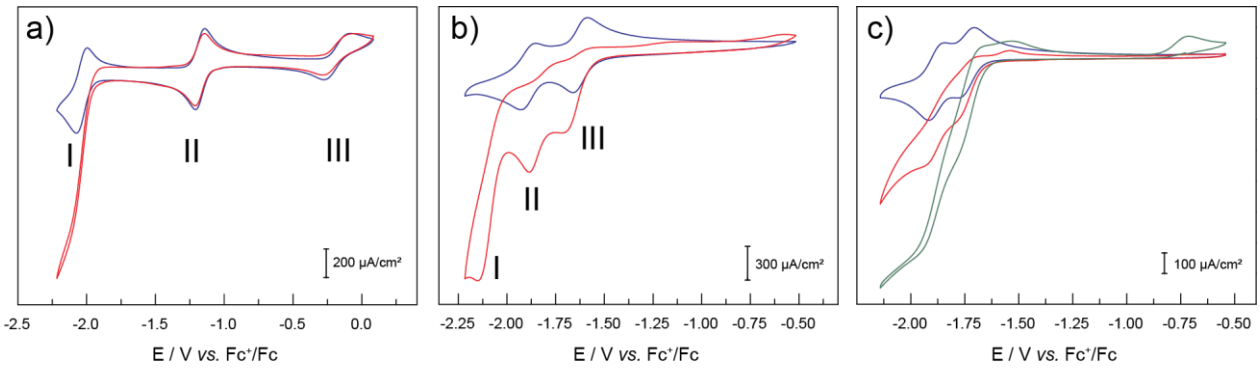

Fig. 1 Typical cyclic voltammograms of 2 mM solutions of **Co-tpy** (a) and **Ni-tpy** (b) under argon (blue) and CO_2 (red) atmospheres at 100 mV/s. c): cyclic voltammograms at 100 mV/s of a 1 mM solution of **Zn-tpy** in DMF/H_2O (90:10, v:v) under argon (blue, only the third scan is presented), CO_2 (red, only the third scan is presented), and under CO_2 after the addition of over 20 mM excess tpy ligand (green, only the third scan is presented).

potentials (–2.15 V *vs.* Fc^+/Fc), which is absent under Ar (Figure 1b, I).

Cu-tpy

Evidence for deposition behaviour on glassy carbon electrode under CO_2 was observed during cyclic voltammetry experiments of 2 mM **Cu-tpy** solutions in DMF with 5% H_2O (Figure S5). This heterogeneous behaviour is under further investigation and falls outside the scope of this paper.

Fe-tpy and Mn-tpy

Typical cyclic voltammograms of **Fe-tpy** and **Mn-tpy** are shown in the supplementary information (Figure S6). Under the conditions used, no strong current enhancement upon addition of CO_2 on the cyclic voltammetry responses was observed. This suggests a lack of electrocatalytic activity in the conditions tested, in contrast to previous reports as far as **Fe-tpy** is concerned, and these complexes were not investigated further.[26]

Zn-tpy

The typical voltammogram of a 2 mM solution of **Zn-tpy** exhibits two reversible electrochemical features, at –1.68 and –1.81 V *vs.* Fc^+/Fc (Figure 1c). Since the reduction of Zn^{II} to Zn^{I} is not likely to occur under these conditions, the two waves are assigned to ligand-based reduction processes. The two electrochemical features become irreversible and the intensity of the corresponding cathodic peaks significantly increase upon addition of CO_2. It has to be noted that a passivation of the glassy carbon electrode was observed as the number of scans was increased (Figure S7). As shown in Figure 1c, the intensity of the cathodic peaks is further increased upon addition of an excess of tpy ligand. When the same solution, containing excess tpy, is saturated with Ar, the two waves of **Zn-tpy** become reversible once more, with no visible contribution of additional equivalents of tpy to the current observed.

Controlled-potential electrolyses

In order to assess the catalytic activity of the various **M-tpy** complexes under study and to characterize the catalyzed reaction, controlled-potential electrolysis of CO_2-saturated DMF/H_2O (95:5, v:v) with 0.1 M TBAP solution of each complex were carried out. Quantitative analyses of CO and H_2 formation were achieved by gas chromatography, formaldehyde (HCHO) formation by a colorimetric assay and formic acid (HCOOH) formation by ion-exchange chromatography coupled to a conductimeter, as described in the experimental section. The presence of methane was assessed through gas chromatography, of methanol by ^1H and ^{13}C NMR and of oxalate by ionic exchange chromatography. Formaldehyde, methane, methanol and oxalate could not be detected in any of the following experiments.

Co-tpy

Electroreduction of CO_2 in the presence of 2 mM of **Co-tpy** results in the exclusive formation of CO and H_2 (in some cases tiny amounts of formate are also detected, always < 3% of the charge passed, but are attributed to deleterious reactions of DMF). Controlled-potential electrolysis at –2.03 V yields sustained current over the course of 3 hours. During the first hour of the electrolysis, a decrease in the current is observed while the first 1.93 C are exchanged before reaching the steady value of –0.39 mA. This charge corresponds to about $2{\cdot}10^{-5}$ moles of electrons and is attributed to the first quantitative one-electron reduction of Co^{II} to Co^{I} prior to the formation of the catalytic species. Cyclic voltammograms of the bulk solution after a 3h electrolysis exhibit the same features as that of **Co-tpy**, but the open circuit potential was more negative than –1.17 V, indicating that most of the **Co-tpy** species in solution was formally Co^{I}. The production of CO and H_2 was constant over time in the region where the current densities are stable, (Figure S8), corresponding to 17% faradic yield (12% for CO and 5% for H_2).

In the absence of **Co-tpy**, a steady low background current of 19 µA was observed, with background levels of CO ($1.6{\cdot}10^{-8}$ moles) and H_2 (< $6{\cdot}10^{-7}$ moles) being formed after 3h. Electrolysis of **Co-tpy** for 3h in N_2 saturated solution, in the absence of CO_2, resulted in a continuous decrease of the current to levels observed without catalyst. At the end of the 3h electrolysis, 3.31 C were passed, corresponding to slightly under 2 equivalents of electrons per **Co-tpy** molecule. Background levels of CO and H_2 were detected during this experiment. In the absence of water, lower faradic yields, lower current and fewer moles of CO were observed (Figure S9). These experiments combined indicate that CO_2

reduction in this system requires the

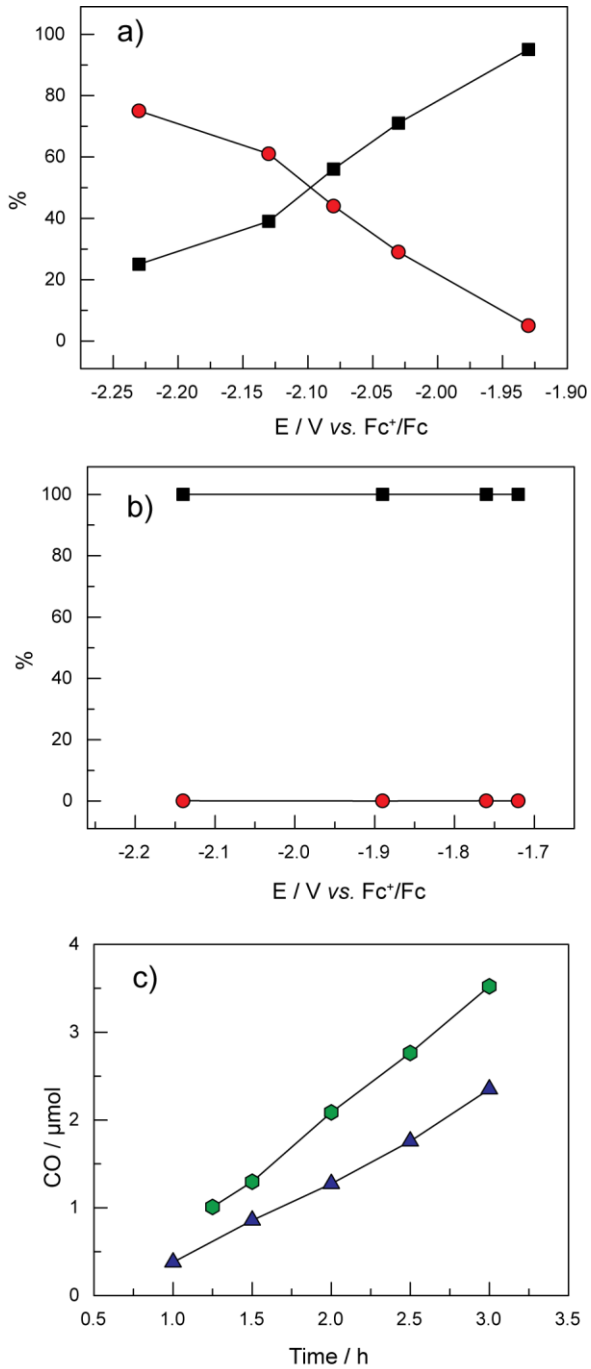

Fig. 2 Evolution of the proportions of CO (black squares) and H_2(red circles) among the products observed for CO_2 reduction by **Co-tpy** (a) and **Ni-tpy** (b) with the applied potential during controlled-potential electrolyses. c): comparison of the number of moles of CO produced by **Ni-tpy** (green hexagons) and **Co-tpy** (blue triangles) during the course of 3h electrolyses at -1.72 V for **Ni-tpy** and -1.93V for **Co-tpy**. Carbon monoxide generation by the **Ni-tpy** system is better in these conditions than for **Co-tpy**, even at a 200 mV less overpotential (lines drawn to guide the eye).

Co-tpy complex, CO_2, and a proton source such as water.

The influence of the applied potential on product distribution was investigated by varying the applied potential in controlled-potential electrolysis experiments. Five different potentials were tested, in the range of –1.93 to –2.23 V *vs.* Fc^+/Fc. At all applied potentials tested, the current densities decrease during the first 30 minutes to 1h (depending on the potential) corresponding in each case to about 1.93 C before reaching a steady current density (Figure S10). The stable current densities values increase upon decreasing the applied voltage (from –0.29 mA at –1.93 V to –1.28 mA at –2.23 V). The relative amounts of H_2 and CO formed vary with the applied voltage, with the highest CO:H_2 ratio value of 20 obtained at –1.93 V (Figure 2a). The CO:H_2 ratio decreases to 0.3 as the applied potential was lowered to –2.23 V *vs.* Fc^+/Fc, thus allowing a simple control of the produced CO/H_2 mixture by the potential applied during electrolysis. The combined faradic efficiency going towards CO and H_2 was between 16-21%, with little variation as the applied potential was varied.

Several routes were explored to account for the low faradic efficiency going towards CO_2 reduction products. First the influence of solvent was investigated. To reduce reactivity of the methyl groups of DMF, *N*,*N*-diethylformamide (DEF) was tested as a solvent and 1-methyl-2-pyrrolidinone (NMP) was tested to reduce the potential interference from reaction with the carbonyl group. These solvent variations lead to similar faradic yields for CO and H_2 production (Figure S11). The influence of the electrolyte on the low faradic yields was also investigated. Sequential modifications of the cation from TBA^+ to Li^+ and of the anion from ClO_4^- to PF_6^- also lead to similar faradic efficiency (data not shown). Since **Co-tpy** is also known for O_2 reduction catalysis, the influence of potential O_2 leaks in the system during bulk electrolysis was investigated by performing the experiment in a N_2 filled glovebag. No significant influence on faradic yields was observed. Finally, as shown below, faradic yields increase upon decreasing tpy:Co ratios, during electrolysis of mixtures of tpy and $CoCl_2$ and greatly decrease upon addition of an excess of bipyridine (table 1). All these results are consistent with the speculation that the low faradic efficiencies for CO_2 reduction results from the pyridine rings of the ligands being involved in side reactions under these conditions.

Ni-tpy

As shown by the cyclic voltammetry experiments, the onset potential for electroreduction of CO_2 catalyzed by the **Ni-tpy** system is less negative than in the **Co-tpy** system. Thus, electrolyses can be carried out at applied potentials as positive as –1.72 V, more than 200 mV less negative than that required for electroreduction of CO_2 catalyzed by **Co-tpy**. Two major features differentiate the Ni-tpy system from the **Co-tpy** system: (i) larger but significantly less stable current densities at any applied potential from –1.72 to –2.14 V and (ii) formation of CO as the unique reaction product, since no H_2 could be detected (Figure 2b). However as in the case of **Co-tpy**, we could not account for the total charge, since a Faradic yield of 20% at best was obtained with no effect of varying the applied potential (Figure S12). As with the **Co-tpy** system, ligand reactivity is proposed to explain at least in part the low yield. The two systems are compared in Figure 2c, in terms of CO production, which shows that under similar conditions CO production is more efficient in the case of the **Ni-tpy** system.

Zn-tpy

Controlled-potential electrolysis of a 5 mM solution of **Zn-tpy** at –2.15 V vs. Fc^+/Fc in CO_2-saturated conditions exhibits a current of about –1.8 mA, which slowly decreases, as in the **Ni-tpy** case, to reach about –0.8 mA after 3h (Figure S13). Notably, no corresponding CO_2 reduction products or H_2 could be detected.

The paramagnetic nature of the cobalt and nickel based systems precluded investigations of degradation pathways through ^1H NMR, but the diamagnetic nature of Zn^{II} allowed us to probe these side reactions. Assuming that Zn^{II} catalyses the same side reactions responsible for the low faradic efficiency observed for **Ni-tpy** and **Co-tpy** under CO_2-saturated conditions, the system was studied further.

Bulk electrolyses of 4 mM solutions of terpyridine in the absence of Zn^{II} at –2.03 V or at –2.23 V *vs.* Fc^+/Fc under CO_2 lead to significant steady currents (–0.13 mA at –2.03 V and –0.45 mA at –2.23 V), contrary to what is observed under inert atmosphere (Figure S14). No CO_2 reduction products or H_2 can be detected in these experiments as was the case for electrolysis of **Zn-tpy** solutions in the presence of CO_2. This suggests the possibility that tpy transformation is a significant side reaction during catalysis that limits faradic efficiencies.

To experimentally probe the hypothesis of tpy being involved in side reactions we investigated **Zn-tpy** as a diamagnetic version of the system during both electroreduction and photoreduction of CO_2, with the aim of using ^1H NMR spectroscopy to get some insight into the production of tpy-derived compounds. Photochemical reduction is considered as it provides the opportunity to generate larger concentrations of such compounds more rapidly. Literature precedents suggest that in DMF, under CO_2, at reducing potentials, *N*-heteroaromatic cycles can undergo *N*-carboxylation reactions to yield compounds that can be trapped by addition of alkylating agents.[30] In a first series of experiments a 5 mM **Zn-tpy** solution was electrolysed at –2.15 V during 4.5 h. Iodomethane was then added to the solution which was stirred at room temperature for 1.5 h. ^1H NMR of the resulting solution is consistent with a carboxylation reaction (see Figure S13 for experimental details). In a second series of experiments **Zn-tpy** was photolysed in the presence of CO_2 and $[Ru(bpy)_3]^{2+}$ as the photosensitizer in MeCN/TEOA (triethanolamine, the sacrificial electron donor) and the resulting solution was analyzed by ^1H NMR (Figure S15). The ^1H NMR spectrum shows the presence of protons in the aliphatic region which are not originating from TEOA degradation pathways. This suggests a loss of aromaticity on the pyridine rings of the ligands and direct transformation of tpy. All these observations further support these pathways as contributing to the low faradic efficiencies of the reaction of **M-tpy** with CO_2.

Mechanism probing and turnover frequencies

Further analyses of the cyclic voltammetry data were performed in order to obtain some insight into the mechanistic pathway for CO_2 reduction with the **Co-tpy** system. The reaction order in **Co-tpy** was initially established via analysis of the catalytic peak current densities observed by cyclic voltammetry. The catalytic peak current varies linearly with the catalyst concentration (Figure S16), consistent with a mechanism for CO_2 reduction that is first order in cobalt under these conditions on the CV time scale. An apparent pseudo-first order rate constant of 10.4 s^{-1} was obtained using the *foot-of-the-wave* analysis proposed by Savéant and co-workers,[31] applied to the cyclic voltammetry data

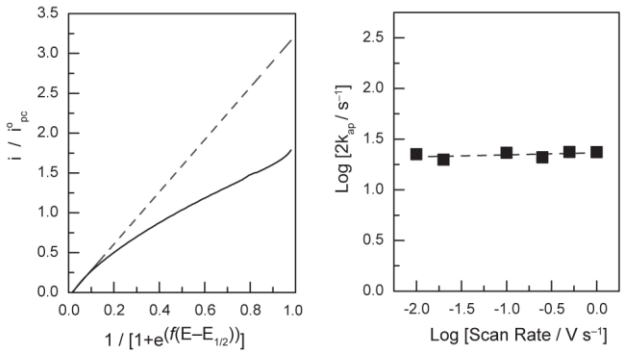

Fig. 3 *Foot-of-the-wave* analysis on the **Co-tpy** system at 250 mV/s (left), *f=F/(RT),* and plot of log($2k_{ap}$) as a function of scan rate (right).

collected exclusively with a **Co-tpy** concentration equal to 2.0 mM. The details of the analysis can be found in the SI. As expected when the assumptions of the *foot-of-the-wave* analysis are met, this rate constant is virtually invariant with respect to two orders of magnitude of scan rate analysed (Figure 3, right).

Under the experimental conditions used, one can estimate a turnover frequency of about $3.2 \cdot 10^{-10}$ s^{-1} at zero overpotential for the production of CO, which is within an order of magnitude to that which has been reported for other polypyridyl based CO_2 reduction catalysts of various transition metals.[32] In this calculation, the CO/CO_2 reduction potential in a DMF/water solvent mixture is estimated to be –1.41 V *vs.* Fc^+/Fc, as the CO/CO_2 potential is reported to be –0.690 V *vs.* NHE[32] and the Fc^+/Fc potential is reported to be 0.720 V *vs.* NHE in DMF.[33] The catalytic cyclic voltammograms of **Co-tpy** display substantial current enhancement with an applied potential of –2.08 V *vs.* Fc^+/Fc, which represents an applied overpotential of 0.67 V. This overpotential can be factored into the TOF calculation and a TOF within the catalytic wave was determined to be 74 s^{-1}.

Deviations of the experimental data from the idealized s-shaped catalytic activity curve within the *foot-of-the-wave* analysis begin very soon after the onset of catalytic activity (Figure 3, left). Qualitatively, the strong deviations observed are in agreement with either fast substrate consumption or product inhibition of catalysis. Despite our inability to conclusively differentiate between the types of deviations, the relatively low intrinsic catalytic activity of **Co-tpy** suggests that fast substrate consumption (faster than rates of substrate diffusion) is not likely the cause of the deviation being observed, thus making fast product inhibition the likely cause of the deviation for idealized behaviour.

Controlled-potential electrolyses experiments were also used to gain an insight into the mechanism. Bulk electrolysis at a fixed applied potential of –2.03 V were carried out on solutions of **Co-tpy** at different concentrations in order to assess the order of **Co-tpy** under steady state conditions as opposed to fast time scales previously probed by CV experiments. The faradic yields for CO and H_2 production were constant in the range of concentration tested. The potential was also varied in a step-wise manner. The results, as shown in Figure S17, indicate that under steady-state bulk electrolysis conditions the apparent order in cobalt was 0.5 at

the 5 potentials tested between in the –1.97 to –2.07 V potential range. The order then increased to 0.74 as the potential was further decreased to more negative values, probably because of less stable current densities. Of importance is that the order in **Co-tpy** was found to be 1 under the fast time scale conditions of a CV experiment (Figure S16) but was found to definitely be less than 1 (likely 0.5) under steady state conditions. This difference is attributed to an inhibition process that occurs under steady state conditions and will be elaborated upon within the Discussion Section.

A plot of potential *vs.* the log of the total current, a Tafel plot, at various catalyst concentrations was extracted from the experimental bulk electrolysis data. The data are shown in Figure S18. At all concentrations, linearity was observed over a short range of potentials from –1.9 to –2.1 V with a slope of 135 mV/dec. This slope of approximately 120 mV/dec is indicative of rate limiting electron transfer from the electrode. As the potential is stepped to more negative values, the slope increases rapidly to reach values > 1 V/dec. This supports either a chemical rate determining step or mass transport limitation to the apparent kinetics. The lack of a pre-equilibrium electron transfer step inhibits our ability to utilize electrochemistry to probe further into mechanistic aspects of electrocatalytic reduction of CO_2 by **Co-tpy**.

Since there are no available coordination sites for interaction with CO_2 in $[Co(tpy)_2]^+$, it was assumed that a catalytic species different from the starting complex was generated during bulk electrolysis resulting from either decoordination of a pyridine ring of tpy or complete loss of a tpy ligand. In order to assess the ligand-to-metal stoichiometry of the catalytically relevant species, a methodology used by Sauvage and Lehn[34] in the study of CO_2 photo-reduction by the analogous $[M(bpy)_n]^{m+}$ complexes was followed, in which the efficiency of the catalysis, during bulk electrolyses, was assessed while the tpy:Co ratio was varied by combining tpy with $CoCl_2$ salt. The results, in terms of the faradic efficiency for CO production, are summarized in table 1 (additional data provided in Figure S19).

Table 1: influence of the relative concentrations (mM) of tpy, $CoCl_2$ and bpy and of time on CO faradic yields ($\%_{CO}$) observed during bulk electrolyses at –2.03 V *vs.* Fc^+/Fc.

tpy	bpy	$CoCl_2$	$\%_{CO}$ 1h-2h	$\%_{CO}$ 2h-3h
4	0	2	7	6
2	0	2	38[a](76[b])	11
2	2	2	8	3
2	0	0	0	0
1	0	2	46	16
0	0	2	1	4

[a:] Measured between minutes 45 and 90 of electrolysis.[b.] Measured between minutes 45 and 60 of electrolysis.

At –2.03 V *vs.* Fc^+/Fc, solutions of 2 mM $CoCl_2$ appear to exhibit electrocatalytic activity. This system is highly unstable, as the current intensity continuously decreased down to baseline levels during the 3h electrolysis, and produced almost exclusively H_2 with only traces of CO (data not shown). This is attributed to the formation of Co^0 nanoparticles which can be rendered electrochemically inert via amalgamation with the mercury, thus explaining the constant drop in current densities. When solutions of terpyridine are electrolyzed at –2.03 V under CO_2, a steady current is observed but no CO or H_2 could be detected. As the tpy:Co ratio is decreased, faradic efficiencies for CO production are increased, with the highest recorded value of 76% during the beginning of the electrolysis of a 1:1 Co/tpy mixture. These results tend to suggest a catalytic species composed of at most 1 equivalent of terpyridine per cobalt centre.

Discussion

Polypyridyl-supported metal compounds have been extensively utilized in the electrocatalytic reduction of CO_2, with $[Re(^tBu\text{-}bpy)(CO)_3Cl]$ and $[Ru(tpy)(bpy)(solvent)]$ being the most efficient and well-studied catalysts, among others.[16,22,35,36] All of these compounds have been shown to catalyze the reduction of CO_2 to carbon monoxide or formate, and in most cases H_2 was observed as well. Despite the success of such polypyridyl-supported noble metal catalysts, fewer examples of first row transition metal polypyridyl-based CO_2 reduction electro-catalysts are present in the literature, with the most active ones being based on variations of the $[Mn(bpy)(CO)_3Br]$ catalyst developed by Deronzier and collaborators.[22,23]

In all of these cases, the polypyridine backbone was advantageous due to its redox active nature and thus should be considered as a non-innocent ligand.[18,21,37] Multiple equivalents of electrons are thus able to be stored on such catalysts, which facilitates multi-electron reactivity with CO_2, avoiding the highly energetic one-electron reduction of CO_2 to $CO_2^{\bullet-}$.[38] The reduced polypyridyl rings act as the reservoir of electrons for CO_2 reduction, and the metal centre mediates the transfer of these reducing equivalents to CO_2.

We sought to gain general insight into the electrocatalytic behaviour of meridionally coordinated terpyridine 3d transition metal complexes by revisiting work initiated by H. D. Abruna, albeit in a different context.[25,26,27,28] Although the initial reports indicate a possible activity of the Cr-tpy derivatives,[28] we focused our attention on late transition metals, seeking to understand underlying differences in the reactivity of the Co and Ni derivatives specifically, as well as gleaning insight into the general reaction mechanism.

The central role of ligand reduction in mechanisms postulated for polypyridyl-based CO_2 reduction catalysts highlights the importance of understanding the reduction potential assignments within the cyclic voltammetry experiments. The assignments of the waves in the cyclic voltammograms of the **M-tpy** complexes are the subject of multiple differing interpretations. Originally, in the case of **Ni-tpy** the two reduction waves (Figure 1b, III and II) were assigned as metal-based and ligand-based, respectively.[26,27] We have found, by comparison with **Zn-tpy**, that the waves would be better described as both being ligand-based. This is further supported by recent studies on the electronic structure of Ni monoterpyridine and $[Ni(tpy)_2]^{2+}$ compounds.[39,40] In contrast, in the case of **Co-tpy**, reduction of the ligand occurs at potentials more negative than those required to generate the Co^I species.

These assignments have implications on the electronic structure of the catalytic species and point to a possible significant difference between the Co and Ni-based catalysts: during

controlled-potential electrolysis, the bulk solution mostly contains Co^{I} in the **Co-tpy** case, but Ni^{II} in the **Ni-tpy** case. This has a strong impact on the possible mechanistic pathways. Co^{I} centres have been shown to lead, upon reaction with protons, to the formation of a Co^{III}-H which would then be implicated in H_2 evolution,[41,42,43,44,45,46] which has been demonstrated in related

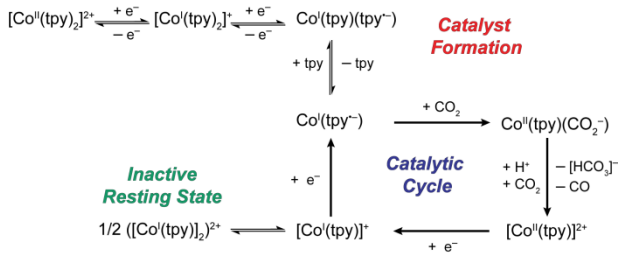

Scheme 2 Proposed mechanism for CO_2 reduction to CO by **Co-tpy**.

polypyridyl-based cobalt complexes as well.[47,48,49] This is in sharp contrast with the Ni-based system, since a Ni^{IV}-H resulting from the protonation of a Ni^{II} centre is unlikely to form in the conditions of the experiment.[50,51,52,53] This would explain the distinct difference in reactivity of the two catalytic systems in terms of product distribution, since metal hydrides are required for H_2 evolution but are not necessarily needed for CO_2 reduction, and are often not invoked in the specific case of CO_2 reduction to CO. Thus, as confirmed herein, **Co-tpy** is more susceptible than **Ni-tpy** to proton reduction, in parallel to conversion of CO_2 into CO. However, we showed that the selectivity of the reaction in the case of **Co-tpy** can be easily tuned upon varying the applied voltage (Figure 2a). Indeed, at the lowest potentials electrolysis generated CO almost exclusively, while decreasing the potential resulted in a drop of the CO:H_2 ratio, with a CO:H_2 value of 1 at about –2.1 V.

To allow for direct interaction between CO_2 and the metal centre, the ability of the system to liberate a coordination site is crucial. This is achieved in Ru-based catalysts[35] by the exchange of a solvent molecule for CO_2, in $[M(bpy)_3]$ compounds by the prior loss of a bpy ligand[54] and in the case of $[Re(bpy)(CO)_3Cl]$ the opening of a coordination site through loss of the Cl ligand is triggered by bpy reduction.[55] Similarly, we propose that ligand reduction triggers the loss of the second (neutral) terpyridine ligand, as supported by the **Ni-tpy** CVs at slow scan rates and as has been proposed for analogous cobalt-based systems.[56]

The proposed mechanism for **Co-tpy** is depicted in Scheme 2, where solvent, electrolytes, or other Lewis bases complete the coordination sphere around the cobalt. We propose that the $[Co^{II}(tpy)_2]^{2+}$ compounds acts as the pre-catalyst. Upon reduction of first Co^{II} to Co^{I} and then tpy to $tpy^{\bullet-}$, a neutral terpyridine ligand is lost, generating a catalytically active species with a stoichiometry of 1 tpy per Co. In steady state bulk electrolysis conditions however, we propose that a resting state dimeric species forms where two $[Co^{I}(tpy)]$ centres are bridged, possibly by carbonates or carbonyl groups, as has been reported in analogous structures in the literature.[57,58,59,60,61,62] The carbonates could possibly originate either from a CO_2/water equilibrium or as an outcome of CO formation. The necessity for this dimer to break apart, liberating the Co monoterpyridine catalyst, is supported by the apparent order of 0.5 observed in these conditions, as well as the observation from the Tafel data that of a chemical limiting step.

The *foot-of-the-wave* analysis further supports the claim of product inhibition. By analogy with reported mechanism for CO formation on related polypyridine compounds, we propose the substitution of CO_2 for a solvent molecule in the $[Co^{I}(tpy^{\bullet-})]$ entity, which then reacts with a second CO_2 molecule and H^+ to yield a Co-CO intermediate, which eventually releases CO and HCO_3^-. This mechanism for CO generation likely can be extended to **Ni-tpy**, however the two catalytically relevant reduction events for the catalyst would be primarily ligand based.

An alternate pathway, paralleling CO and H_2 formation, explains the low Faradic yield. It is likely that the reduction of the tpy ligand renders it highly susceptible to further reactions, such as carboxylations,**Erreur ! Signet non défini.** or possibly hydrogenation[18], which compete with CO and H_2 formation. Previous reports in the case of noble metal-based systems have also pointed to such a parallel process that might explain the low faradic yields.[17,18] However it seems that the late first row transition metals are less efficient in avoiding these reactions as faradic yields for CO+H_2 are significantly lower in that case.

Experimental section

General considerations

M-tpy compounds were synthesized according to modified literature procedures.[26,63,64] Hexadistilled mercury used for bulk electrolyses was purchased from Ophram. Annealed platinum wire was purchased from Alfa Aesar. Anhydrous solvents (*N*,*N*-dimethylformamide, *N*,*N*-diethylformamide, 1-methyl-2-pyrrolidinone and acetonitrile), tetra-*n*-butylammonium perchlorate, lithium perchlorate, tetra-*n*-butylammonium hexafluorophosphate, cobalt(II) chloride, zinc chloride, nickel(II) chloride, manganese(II) perchlorate hydrate, iron(II) chloride, copper(II) chloride, iodomethane, tris(2,2′-bipyridyl)dichlororuthenium(II) hexahydrate, triethanolamine, 2,2′:6′,2″-terpyridine, 2,2′-bipyridyl, acetonitrile-d_3 and deuterium oxide were purchased from Sigma-Aldrich and used as received. ^{1}H NMR was performed on a Brücker 300 MHz instrument.

Cyclic voltammetry experiments

All cyclic voltammetry experiments were carried out in a single-compartment cell using a 1 mm diameter glassy carbon electrode (from Bio-Logic) unless otherwise noted. The electrode was polished before each measurement with a 1 µm diamond suspension. A Pt wire counter electrode was used, with a Ag/AgCl, 3M KCl reference electrode separated from the solution by a Vycor tip. IR drop was compensated to 85% using the ZIR built-in compensation method of the SP 300 Bio-Logic potentiostat used.

All electrochemical data were referenced to the potential of the Fc^+/Fc couple in the solvent system used. The IUPAC convention was used to report current. The supporting electrolyte used was tetrabutylammonium perchlorate (TBAP) at a concentration of 0.1 M in DMF/H_2O mixtures. All solutions were purged with inert gas (N_2 or Ar) or CO_2 for at least 15 minutes before CVs were recorded. Unless otherwise noted, at least 10 superimposable scans were recorded for each experiment to insure the equilibrium was reached.

Controlled-potential electrolyses

Bulk electrolysis experiments were carried out in a custom made

two-compartment cell (Figure S20). A 1.5 cm diameter pool of mercury was used as working electrode unless otherwise noted. The counter electrode used was a platinum wire separated from the working electrode by a porous 4 frit, and an Ag/AgCl, 3M KCl reference electrode was separated from the solution by a Vycor tip. The volume of solution used in the working compartment of the cell is 10 mL, and the typical headspace volume is 31 mL. No IR compensation was done for bulk electrolyses. A Bio-Logic SP 300 potentiostat connected to a booster card was used to apply potential and record charge and current. Bulk electrolysis solutions were purged with inert gas or CO_2 for 15 min prior to electrolysis. Solutions were constantly stirred throughout bulk electrolysis experiments.

Chemical analysis

H_2 measurements were performed by gas chromatography on a Shimadzu GC-2014 equipped with a Quadrex column, a Thermal Conductivity Detector and using N_2 as a carrier gas. CO was measured using a Shimadzu GC-2010 Plus gas chromatography, fitted with a Restek Shin Carbon column, helium carrier gas, a methanizer and a Flame Ionization Detector. Gas chromatography calibration curves were made by sampling known volumes of CO and H_2 gas respectively. The typical volume of gas injected was 50 µL. The presence of CH_4 was assessed using the same set-up.

Formate and oxalate concentrations were determined using a Metrohm 883 Basic IC plus ionic exchange chromatography instrument, using a Metrosep A Supp 5 column and a conductivity detector. A typical measurement requires the sampling of 1 mL of solution, followed by a 100 fold dilution in deionised 18 MΩ/cm water and injection of 20 µL into the instrument. Caution is necessary when determining formate concentrations if DMF is being employed as a solvent. Great care must be taken to separate the counter electrode from the working electrode as formate is generated at the counter electrode through one-electron oxidation of DMF followed by hydrolysis.

Formaldehyde concentration was determined using the Nash colorimetric test[65] using a Shimadzu UV-1800 instrument. We observed that post-electrolysese solutions containing DMF and **Co-tpy** must be analysed for formaldehyde quickly as reoxidation in air led to increasing amounts of formaldehyde being produced, which is attributed to the reaction of DMF with a Co^{III}-tpy, generated through the reaction of **Co^{II}-tpy** with O_2.

Methanol presence was assessed using a Shimadzu GC-2010 Plus gas chromatography fitted with a ZB-WAX Plus column, Helium as a carrier gas and a flame ionization detector. MeOH presence was also assessed through ^{1}H NMR spectroscopy on a Brücker 300 MHz Instrument.

Conclusions

We have shown that homoleptic terpyridine complexes of nickel and cobalt are competent catalysts for the electrocatalytic reduction of CO_2 to CO as the exclusive carbon containing product. The catalysis is observed to begin by reduction of a tpy ligand for both the **Ni-tpy** and **Co-tpy** systems. The systems differ in that the resting state of the **Co-tpy** catalyst is assigned to be monovalent cobalt whereas the resting state of the **Ni-tpy** catalyst is assigned to be divalent nickel. The higher valent nickel catalyst is proposed to be unable to generate intermediate nickel-hydrides required for hydrogen generation in the conditions used and thus exhibits remarkable selectivity for CO_2 reduction to CO over proton reduction. The lower valent cobalt catalyst is found to generate gaseous mixtures of CO and H_2, the ratio of which can be tuned base on the overpotential which is applied. Decomposition of the polypyridyl ligand has been shown to be the primary pathway which limits overall faradic efficiency, even though the intrinsic catalytic activity for the cobalt based system is comparable to that which has been reported for other metal-polypyridyl catalysts.

Acknowledgements

We acknowledge support from Fondation de l'Orangerie for individual Philanthropy and its donors and from the French National Research Agency (ANR, Carbiored ANR-12-BS07-0024-03). This work was supported by the French State Program 'Investissements d'Avenir' (Grants "LABEX DYNAMO", ANR-11-LABX-0011-01 and LABEX ARCANE, ANR-11-LABX-0003-01). The authors would like to thank Dr. P. Simon for efforts towards the development of initial detection methods for formate through a colorimetric coupling method and of formaldehyde through a chromotropic acid test and J. P. Porcher for initial help with setting-up H_2 measurements. N. E. acknowledges the Direction Générale de l'Armement (DGA) for a graduate research fellowship.

Notes and references

[a] *Laboratoire de Chimie des Processus Biologiques, UMR 8229 CNRS, Université Pierre et Marie Curie – Paris 6, Collège de France, 11 Place Marcelin Berthelot, 75231 Paris Cedx 05, France. Fax: +33 1 44271356; Tel: +33 1 44271360; E-mail : marc.fontecave@cea.fr*

[b] *Laboratoire de Chimie et Biologie des Métaux, Université Grenoble Alpes, CNRS UMR 5249, CEA, 17 avenue des martyrs, 38054 Grenoble Cedex 9, France. Tel: +33 4 38789122*

† Electronic Supplementary Information (ESI) available: additionnal information as noted in the text. See DOI: 10.1039/b000000x/

1 N. S. Lewis and D. G. Nocera, *Proc. Natl. Acad. Sci.*, 2006, **103**, 15729.

2 T. Faunce, S. Styring, M. R. Wasielewski, G. W. Brudvig, A. W. Rutherford, J. Messinger, A. F. Lee, C. L. Hill, H. deGroot, M. Fontecave, D. R. MacFarlane, B. Hankamer, D. G. Nocera, D. M. Tiede, H. Dau, W. Hillier, L. Wang and R. Amal, *Energy Environ. Sci.*, 2013, **6**, 1074.

3 T. R. Cook, D. K. Dogutan, S. Y. Reece, Y. Surendranath, T. S. Teets and D. G. Nocera, *Chem. Rev.*, 2010, **110**, 6474.
4 H. Arakawa, M. Aresta, J. N. Armor, M. A. Barteau, E. J. Beckman, A. T. Bell, J. E. Bercaw, C. Creutz, E. Dinjus, D. A. Dixon, K. Domen, D. L. DuBois, J. Eckert, E. Fujita, D. H. Gibson, W. A. Goddard, D. W. Goodman, J. Keller, G. J. Kubas, H. H. Kung, J. E. Lyons, L. E. Manzer, T. J. Marks, K. Morokuma, K. M. Nicholas, R. Periana, L. Que, J. Rostrup-Nielson, W. M. H. Sachtler, L. D. Schmidt, A. Sen, G. A. Somorjai, P. C. Stair, B. R. Stults and W. Tumas, *Chem. Rev.*, 2001, **101**, 953.
5 J. L. Inglis, B. J. MacLean, M. T. Pryce and J. G. Vos, *Coord. Chem. Rev.*, 2012, **256**, 2571.
6 M. Rakowski DuBois and D. L. DuBois, *Acc. Chem. Res.*, 2009, **42**, 1974.
7 E. E. Benson, C. P. Kubiak, A. J. Sathrum and J. M. Smieja, *Chem. Soc. Rev.*, 2009, **38**, 89.
8 A. J. Morris, G. J. Meyer and E. Fujita, *Acc. Chem. Res.*, 2009, **42**, 1983.
9 A. Winter, G. R. Newkome, U. S. Schubert, *Chem. Cat. Chem.*, 2011, **3**, 1384.
10 C. Kaes, A. Katz and M. W. Hosseini, *Chem. Rev.*, 2000, **100**, 3553.
11 J.-M. Savéant, *Chem. Rev.*, 2008, **108**, 2348.
12 C. C. Scarborough, K. M. Lancaster, S. DeBeer, T. Weyhermüller, S. Sproules and K. Wieghardt, *Inorg. Chem.*, 2012, **51**, 3718.
13 M. Wang, J. England, T. Weyhermüller and K. Wieghardt, *Inorg. Chem.*, 2014, DOI: 10.1021/ic4029854.
14 J. Hawecker, J.-M. Lehn and R. Ziessel, *J. Chem. Soc., Chem. Commun.*, 1984, 328.
15 T. Yoshida, K. Tsutsumida, S. Teratani, K. Yasufuku and M. Kaneko, *J. Chem. Soc., Chem. Commun.*, 1993, 631.
16 J. M. Smieja and C. P. Kubiak, *Inorg. Chem.*, 2010, **49**, 9283.
17 C. Caix, S. Chardon-Noblat and A. Deronzier, *J. Electroanal. Chem.*, 1997, **434**, 163.
18 C. M. Bolinger, N. Story, B. P. Sullivan and T. J. Meyer, *Inorg. Chem.*, 1988, **27**, 4582.
19 P. Paul, B. Tyagi, A. K. Bilakhiya, M. M. Bhadbhade, E. Suresh and G. Ramachandraiah, *Inorg. Chem.*, 1998, **37**, 5733.
20 H. Nagao, T. Mizukawa and K. Tanaka, *Inorg. Chem.*, 1994, **33**, 3415.
21 Z. Chen, C. Chen, D. R. Weinberg, P. Kang, J. J. Concepcion, D. P. Harrison, M. S. Brookhart and T. J. Meyer, *Chem. Commun.*, 2011, **47**, 12607.
22 M. Bourrez, F. Molton, S. Chardon-Noblat and A. Deronzier, *Angew. Chem. Int. Ed.*, 2011, **50**, 9903.
23 J. M. Smieja, M. D. Sampson, K. A. Grice, E. E. Benson, J. D. Froehlich and C. P. Kubiak, *Inorg. Chem.*, 2013, **52**, 2484.
24 A. R. Guadalupe, D. A. Usifer, K. T. Potts, H. C. Hurrell, A.-E. Mogstad and H. D. Abruna, *J. Am. Chem. Soc.*, 1988, **110**, 3462.
25 H. C. Hurrell, A. L. Mogstad, D. A. Usifer, K. T. Potts and H. D. Abruna, *Inorg. Chem.*, 1989, **28**, 1080.
26 C. Arana, S. Yan, M. Keshavarz-K, K. T. Potts and H. D. Abruna, *Inorg. Chem.*, 1992, **31**, 3680.
27 C. Arana, M. Keshavarz, K. T. Potts and H. D. Abruna, *Inorg. Chim. Acta*, 1994, **225**, 285.
28 J. A. Ramos Sende, C. R. Arana, L. Hernandez, K. T. Potts, M. Keshevarez-K and H. D. Abruna, *Inorg. Chem.*, 1995, **34**, 3339.
29 A. Paul, D. Connolly, M. Schulz, M. T. Pryce and J. G. Vos, *Inorg. Chem.*, 2012, **51**, 1977.
30 P. Fuchs, U. Hess, H. H. Holst and H. Lund, *Acta Chemica Scandinavica B*,1981, **35**, 185.
31 C. Costentin, S. Drouet, M. Robert and J.-M. Savéant, *J. Am. Chem. Soc.*, 2012, **134**, 11235.
32 C. Costentin, M. Robert and J.-M. Saveant, *Chem. Soc. Rev.*, 2013, **42**, 2423.
33 S. Creager, in *Handbook of Electrochemistry*, ed. C. G. Zoski, Elsevier, Amsterdam, 1st edn, 2007, ch. 3, pp. 101.
34 J.-M. Lehn and R. Ziessel, *Proc. Nati. Acad. Sci. USA*, 1982, **79**, 701.
35 Z. Chen, P. Kang, M.-T. Zhang and T. J. Meyer, *Chem. Commun.*, 2014, **50**, 335.
36 J. Qiao, Y. Liu, F. Hong and J. Zhang, *Chem. Soc. Rev.*, 2014, **43**, 631.
37 J. R. Pugh, M. R. M. Bruce, B. P. Sullivan and T. J. Meyer, *Inorg. Chem.*, 1991, **30**, 86.
38 C. Amatore and J.-M. Saveant, *J. Am. Chem. Soc.*, 1981, **103**, 5021.
39 G. D. Jones, J. L. Martin, C. McFarland, O. R. Allen, R. E. Hall, A. D. Haley, R. J. Brandon, T. Konovalova, P. J. Desrochers, P. Pulay and D. A. Vicic, *J. Am. Chem. Soc.*, 2006, **128**, 13175.
40 C. Hamacher, N. Hurkes, A. Kaiser, A. Klein and A. Schüren, *Inorg. Chem.*, 2009, **48**, 9947.
41 J. L. Dempsey, J. R. Winkler and H. B. Gray, *J. Am. Chem. Soc.*, 2010, **132**, 16774.
42 J. L. Dempsey, J. R. Winkler and H. B. Gray, *J. Am. Chem. Soc.*, 2009, **132**, 1060.
43 J. L. Dempsey, B. S. Brunschwig, J. R. Winkler and H. B. Gray, *Acc.Chem. Res.*, 2009, **42**, 1995.
44 T. Lazarides, T. McCormick, P. Du, G. Luo, B. Lindley and R. Eisenberg, *J. Am. Chem. Soc.*, 2009, **131**, 9192.
45 M. M. Roubelakis, D. K. Bediako, D. K. Dogutan and D. G. Nocera, *Energy Environ. Sci.*, 2012, **5**, 7737.
46 V. Artero, M. Chavarot-Kerlidou and M. Fontecave, *Angew. Chem. Int. Ed.*, 2011, **50**, 7238.
47 R. Ziessel, J. Hawecker and J.-M. Lehn, *Helvetica Chimica Acta*, 1986, **69**, 1065.
48 C. V. Krishnan, N. Sutin, *J. Am. Chem. Soc.*, 1981, **103**, 2141.
49 C. Creutz, H. A. Schwarz, N. Sutin, *J. Am. Chem. Soc.*, 1984, **106**, 3036.
50 Z. Han, L. Shen, W. W. Brennessel, P. L. Holland and R. Eisenberg, *J. Am. Chem. Soc.*, 2013, **135**, 14659.
51 J. Yang, S. E. Smith, T. Liu, W. G. Dougherty, W. A. Hoffert, W. S. Kassel, M. Rakowski Dubois, D. L. Bubois and M. Bullock, *J. Am. Chem. Soc.*, 2013, **135**, 9700.
52 A. D. Wilson, R. H. Newell, M. J. McNevin, J. T. Muckerman, M. Rakowski Dubois and D. L Dubois, *J. Am. Chem. Soc.*, 2006, **128**, 358.
53 J. Y. Yang, R. Morris Bullock, W. J. Shaw, B. Twamley, K. Fraze, M. Rakowski Dubois and D. L. Dubois, *J. Am. Chem. Soc.*, 2009, **131**, 5935.
54 S. Daniele, P. Ugo, G. Bontempelli and M. Fiorani, *J. Electroanal. Chem.*, 1987, **219**, 259.
55 B. P. Sullivan, C. M. Bolinger, D. Conrad, W. J. Vining and T. J. Meyer, *J. Chem. Soc., Chem. Commun.*, 1985, 1414.
56 D. Chen, P.-L. Fabre and O. Reynes, *Electrochimica Acta*, 2011, **56**, 8603.
57 G. Fachinetti, T. Funaioli and P. F. Zanazzi, *J. Chem. Soc., Chem. Commun*., 1988, 1100.
58 E. Fujita, D. J. Szalda, C. Creutz and N. Sutin, *J. Am. Chem. Soc.*, 1988, **110**, 4870.
59 J. Nath, D. Kalita and J. B. Baruah, *Polyhedron*, 2011, **30**, 2558.
60 T. Duangthongyou, C. Phakawatchai and S. Siripaisarnpipat, *Journal of Molecular Structure*, 2011, **987**, 101.
61 K. Dimitrou, K. Folting, W. E. Streib and G. Christou, *J. Am. Chem. Soc.*, 1993, **115**, 6432.
62 S. Bhaduri, N. Y. Sapre and A. Basu, *J. Chem. Soc., Chem. Commun*., 1986, 197.
63 S. Romain, C. Baffert, C. Duboc, J.-C. Leprêtre, A. Deronzier and M.-N. Collomb, *Inorg. Chem.*, 2009, **48**, 3125.
64 U. S. Schubert, C. Eschbaumer, P. Andres, H. Hofmeier, C. H. Weidl, E. Herdtweck, E. Dulkeith, A. Morteani, N. E. Hecker and J. Feldmann, *Synthetic Metals*, 2001, **121**, 1249.
65 S. B. Jones, C. M. Terry, T. E. Lister and D. C. Johnson, *Anal. Chem.*, 1999, **71**, 4030.